Journal of Physics: Conference Series

PAPER • **OPEN ACCESS**

Hard X-ray quiescent emission in magnetars via resonant Compton upscattering

IOP Conf. Series: Journal of Physics: Conf. Series **932** (2017) 012021 doi:10.1088/1742-6596/932/1/012021

Hard X-ray quiescent emission in magnetars via resonant Compton upscattering

M G Baring[1], Z Wadiasingh[2], P L Gonthier[3] and A K Harding[4]

[1] Department of Physics and Astronomy, Rice University, Houston, TX 77251, U.S.A.
[2] Centre for Space Research, North-West University, Potchefstroom, South Africa
[3] Hope College, Department of Physics, 27 Graves Place, Holland, MI 49423, U.S.A
[4] Astrophysics Science Division, Code 663 NASA's Goddard Space Flight Center, Greenbelt, MD 20771, U.S.A.

E-mail: baring@rice.edu

Abstract. Non-thermal quiescent X-ray emission extending between 10 keV and around 150 keV has been seen in about 10 magnetars by RXTE, INTEGRAL, Suzaku, NuSTAR and Fermi-GBM. For inner magnetospheric models of such hard X-ray signals, inverse Compton scattering is anticipated to be the most efficient process for generating the continuum radiation, because the scattering cross section is resonant at the cyclotron frequency. We present hard X-ray upscattering spectra for uncooled monoenergetic relativistic electrons injected in inner regions of pulsar magnetospheres. These model spectra are integrated over bundles of closed field lines and obtained for different observing perspectives. The spectral turnover energies are critically dependent on the observer viewing angles and electron Lorentz factor. We find that electrons with energies less than around 15 MeV will emit most of their radiation below 250 keV, consistent with the turnovers inferred in magnetar hard X-ray tails. Electrons of higher energy still emit most of the radiation below around 1 MeV, except for quasi-equatorial emission locales for select pulse phases. Our spectral computations use a new state-of-the-art, spin-dependent formalism for the QED Compton scattering cross section in strong magnetic fields.

1. Introduction

A topical subset of the neutron star population is defined by magnetars. They are highly-magnetized stars that have historically been divided into two observational groups: Soft-Gamma Repeaters (SGRs) and Anomalous X-ray Pulsars (AXPs). Their extreme fields, which generally exceed the quantum critical value of $B_{\rm cr} = m_e^2c^3/(e\hbar) \approx 4.41 \times 10^{13}$ Gauss (where the electron cyclotron and rest mass energies are equal), are inferred from their X-ray timing properties, presuming that their rapid rotational spin down is due to magnetic dipole torques (e.g. [1]). Such a class of neutron stars with superstrong fields was postulated for SGRs by [2], and for AXPs by [3]. For recent reviews of magnetar science, see [4, 5, 6].

SGRs are transient sources that undergo repeated hard X-ray outbursts. Most of their ephemeral activity consists of short flares of subsecond duration in the 10^{38} erg/sec $< L < 10^{42}$ erg/sec range, often somewhat isolated in time, and sometimes occurring in storms. Yet three magnetars have exhibited giant supersecond flares of energies exceeding 10^{45} ergs: SGR 0525-66 in 1979, as mentioned above, SGR 1900+14 on August 27th, 1998 (e.g. see [7]), and SGR 1806-20 on December 27, 2004 (see [8]). SGRs also exhibit quiescent X-ray emission below 10 keV, of periods P in the range 2–12 sec. (e.g. [1, 9]). The AXPs are bright X-ray sources with periods

in the same range. Their quiescent signals below 10 keV are mostly thermal with steep power-law tails, and possess luminosities $L_X \sim 10^{33} - 4 \times 10^{35}\,\mathrm{erg\ s^{-1}}$ [10].[1] As with the SGRs, these L_X values far exceed their rotational power, perhaps being powered by their internal magnetic energy. Observations of outburst activity in AXP 1E 2259+586 [11], in AXP 1E1841-045 [12] and in others suggest that AXPs and SGRs are indeed very similar. This "unification paradigm" has garnered widespread support within the magnetar community over the last decade. There are also highly-magnetized pulsars that exhibit periods of magnetar-like bursting activity. The observational status quo of magnetars is summarized in the McGill Magnetar Catalog [13].[2]

An additional element of the magnetar phenomenon emerged following the discovery by INTEGRAL and RXTE of hard, non-thermal pulsed spectral tails in three AXPs [14, 15]. These luminous tails are extremely flat, extending up to 150 - 200 keV. Similar quiescent emission tails are seen in SGRs [16, 17]. In various magnetars, a turnover around 500 - 750 keV is implied by constraining *pre-2000* upper limits obtained by the COMPTEL instrument on the *Compton Gamma-Ray Observatory*. The need for such a spectral turnover is reinforced above 100 MeV by upper limits in *Fermi*-LAT data for around 20 magnetars [18, 19]. Magnetic inverse Compton scattering of thermal atmospheric soft X-ray seed photons by relativistic electrons is expected to be extremely efficient in magnetars, and thus is a prime candidate for generating the hard X-ray tails [20, 21]. This paper explores this model, highlighting some recent results from our ongoing program of modeling the resonant Compton hard X-ray emission in magnetars.

2. Hard X-rays in magnetars from magnetic inverse Compton scattering

The scenario for the generation hard X-ray tails considered in this paper is magnetic inverse Compton scattering of thermal atmospheric soft X-ray seed photons by relativistic electrons. This is extremely efficient in highly-magnetized pulsars because the scattering process is resonant at the electron cyclotron frequency and its harmonics, so that there the cross section in the electron rest frame exceeds the classical Thomson value of $\sigma_{\rm T} \approx 6.65 \times 10^{-25}\,\mathrm{cm^2}$ by $\sim 2-3$ orders of magnitude (e.g., [22, 23]). This efficiency is manifested in short cooling lengths, often less than 10^3 cm, for high speed electrons traversing a magnetar magnetosphere [24]. Provided there is a source of electrons with Lorentz factors $\gamma_e \gg 1$, single inverse Compton scattering events can readily produce the general character of hard X-ray tails [20, 21]. In particular, Baring & Harding [20] employed QED scattering cross sections in uniform fields, extending collision integral formalism for non-magnetic Compton upscattering that was developed by [25].

The spectra presented in [20] were characteristically flat, a consequence of the resonant cyclotron kinematics. These do not match observations, nor are they expected to since they integrate over all lines of sight in the uniform $\mathbf{B}$. Non-uniform fields offer a different weighting of angular geometries, and when combined with cooling can steepen the spectrum considerably: see the magnetic Thomson investigation of [26]. In [20], we discerned that kinematic constraints correlating the directions and energies of upscattered photons yielded Doppler boosting and blueshifting along the local magnetic field direction. Therefore, the strong angular dependence of spectra computed for the uniform field case must extend to more complex magnetospheric field configurations. Consequently, emergent inverse Compton spectra in more complete models of hard X-ray tails will depend critically on an observer's perspective and the sampled locales of resonant scattering, both of which vary with the rotational phase of a magnetar. The construction of the resonant Compton upscattering model whose results are presented here is a geometrical extension of the work of [20] to dipolar magnetic field morphologies. Directed emission spectra have been generated for an array of observer perspectives and magnetic inclination angles α to the rotation axis; they serve as a basis for future calculations that

[1] See also the neutron star cooling site `http://neutronstarcooling.info/` for magnetars in a broader context.
[2] An on-line version can be found at `http://www.physics.mcgill.ca/~pulsar/magnetar/main.html`

will treat Compton cooling of electrons self-consistently. The scattering physics employs the state-of-the-art, spin-dependent magnetic Compton formalism developed by us in Gonthier et al. [27] that uses the preferred Sokolov and Ternov eigenstates of the Dirac equation. For details of the model, its kinematics and geometry and spectral characteristics, and their connection to observer perspectives, the reader is referred to the full exposition in Wadiasingh et al. [28].

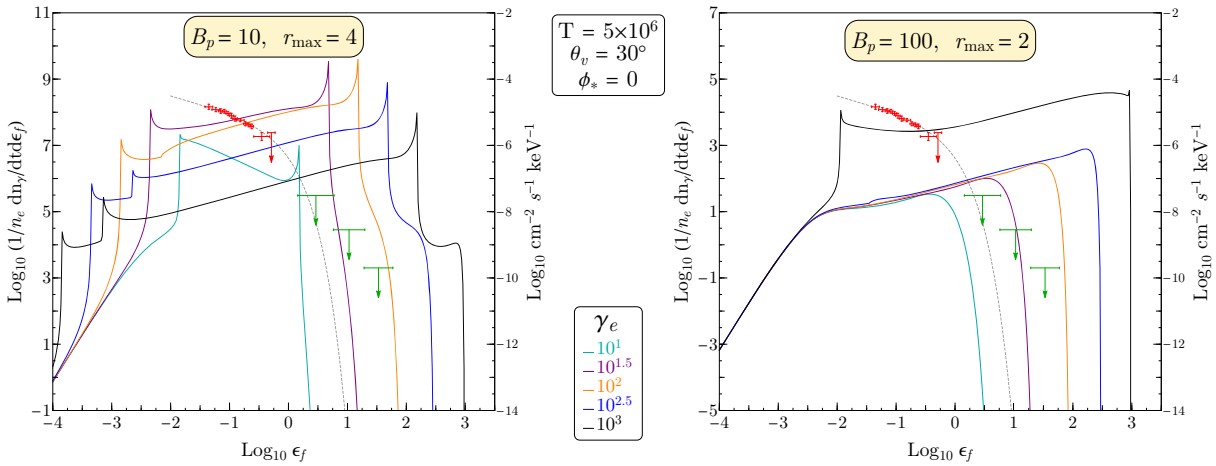

Figure 1. Spectra generated for meridional field loops, those where the line of sight to an observer is coplanar ($\phi_* = 0$) with the loops. The viewing angle of the observer is $\theta_v = 30°$ from the magnetic dipole axis. Results for various electron Lorentz factors are depicted. The left panel illustrates higher-altitude and lower-field directed spectra computed for $B_{\rm p} = 10$ and $r_{\max} = 4$ where the resonant interactions are readily sampled for Lorentz factors $\gamma_e > 10^2$. For the right panel with $r_{\max} = 2$ and $B_{\rm p} = 100$, the local field is much higher, precluding resonant interactions near equatorial regions unless Lorentz factors are much higher. Overlaid on the computed spectra are observational data points for AXP 4U 0142+61 (den Hartog et al. 2008b) along with a schematic $\varepsilon_f^{-1/2}$ power-law with a 250 keV exponential cutoff (black dotted curve).

Two elements of the extensive work in [28] are highlighted here. The first consists of selected but informative spectra, depicted in figure 1, computed for electrons of fixed Lorentz factors traversing individual field lines. They correspond to viewing angles coplanar with the field loops (meridional cases) that readily sample the Doppler boosting and beaming. The combination of γ_e and local field $B \sim B_{\rm p}/r_{\max}^3 \sim \gamma_e \varepsilon_f (1 + \cos\Theta_{Bn})$ essentially controls access to resonant interactions [20], and the value of the spectral index. Here ε_f is the upscattered photon energy in units of $m_e c^2$, and Θ_{Bn} is the observer's angle relative to **B** at the point of scattering. The coupling $B \sim \gamma_e \varepsilon_f (1 + \cos\Theta_{Bn})$ controls the directionality of emitted photons, with higher energies ε_f being beamed closer to the field lines. For much of the range in ε_f, the spectra that sample resonant interactions possess a characteristic scaling $dn/(dtd\varepsilon_f) \sim \varepsilon_f^{1/2}$, i.e. are extremely flat, even harder than the uniform field results in [20]. This approximate power-law dependence is a consequence of kinematics and magnetospheric geometry [28]. Bracketing these quasi-power-law bands are distinctive "horns" or cusps, distinguishing when resonant scatterings are and are not accessed. These appear both at low values ε_f in the soft X-rays/EUV, where they would be dominated by the surface emission signal (not shown), and also in the hard X-ray and gamma-ray domains. The narrow peaks of the horns are weighted images of the resonant differential cross section, enhanced by the beaming. Not all spectra possess frequency ranges where resonant interactions are accessible: for values of local B that are large, resonant interactions in the Wien peak are often not fully sampled, as is evident from computed spectra presented in the right panel of figure 1, and the $\gamma_e = 10$ example in the left panel.

Also illustrated in figure 1 are renormalized hard X-ray spectral data for one magnetar, to illustrate how the monoenergetic electron model from single field loops does not match observations. Modeling of hot thermal surface emission seeded by electron bombardment at loop footpoints is not undertaken. The computed spectra extend beyond the COMPTEL upper limits (green points) when $\gamma_e \gtrsim 30$. Therefore, lower Lorentz factors $\gamma_e \sim 10$ are desirable, and these a naturally generated by electron cooling [24]. High-energy attenuation mechanisms like photon splitting or magnetic pair creation may also be operating. In [28] we also exhibit spectra from integrations over field line azimuths, encompassing the non-meridional loops that dominate the contribution from a toroidal surface comprising dipolar field lines. These demonstrate steeper $dn/(dtd\varepsilon_f) \sim \varepsilon_f^0$ power-laws because the loops that do not provide tangents (i.e. **B** directions) at scattering locales that point toward an observer soften the spectrum. Even more interestingly, [28] illustrate that spectral arrays over such toroidal surfaces that span a range of altitudes yield an envelope that approximately matches the 4U0142+61 spectrum displayed in figure 1, provided that $\gamma_e \sim 10$. This suggests that models with more complete volumetric integrations and electron cooling incorporated will match the spectroscopy of hard X-ray tails.

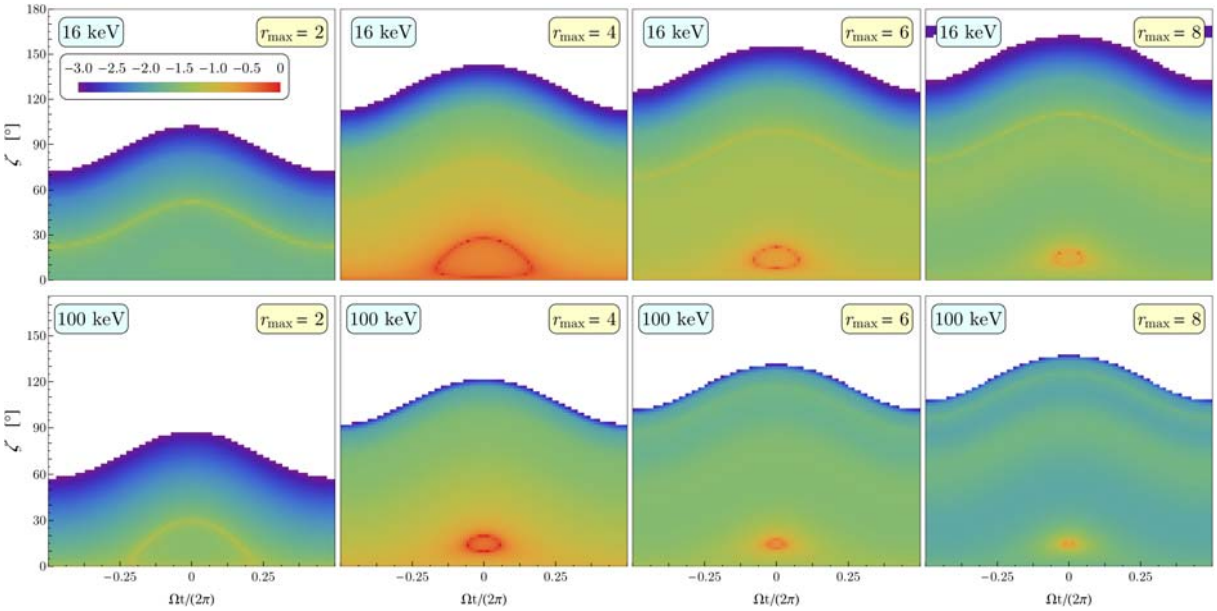

Figure 2. Normalized photon flux $\zeta - \Omega t/2\pi$ phase space maps for resonant Compton upscattering. These represent the logarithmically-scaled (base 10) intensity at energies 16 keV (top row) and 100 keV (bottom row), color coded according to the legend, as a function of spin phase $\Omega t/2\pi$ for each value of ζ on the ordinate. The intensity maps are for uncooled electrons with $\gamma_e = 10^2$, and a uniform surface temperature $T = 5 \times 10^6$ K. They are obtained for azimuthally-integrated bundles of field lines, i.e. a toroidal surface, with $B_p = 10$, and stellar magnetic inclination $\alpha = 15°$, and depict maps for maximum loop altitudes $r_{\max} = 2, 4, 6, 8$. Pulse profiles for a particular observer ζ are represented by horizontal cuts of the maps.

The spectral view so far has been for an instantaneous viewing perspective, i.e. fixed pulse phases. Another element delivered in [28] was the representation of how pulse profiles generated for spectra from toroidal surfaces vary with photon energy ε_f and the maximum surface altitude $r_{\max}$ (in units of $R_{\rm NS}$). These were expressed as sky maps in the $\zeta - \Omega t/2\pi$ plane, and an example is depicted in figure 2. The intensity scale is logarithmic, and is normalized so that the maximum in each row of panels is set to unity. Here, ζ is the angle between the viewer's direction and the magnetar spin axis, and for a particular choice of this angle, horizontal sections within each panel define an intensity trace with pulse phase. Generally, the pulsation profiles are of smooth, single-peaked character. Yet a symmetric double-peak structure of the profiles

in domains $\zeta \approx \alpha$ is evident, being manifested as sections of the red rings: these are realized when quasi-polar viewing is possible at select phases. The phase separation of this double-peak structure in domains $\alpha \approx \zeta$ shrinks at higher $r_{\rm max}$ and larger ε_f. This identifies a potentially potent observational diagnostic: comparing theoretical energy-dependent pulse profiles with observational ones can infer values for α and ζ in magnetars, an analogous protocol to that widely used in gamma-ray pulsar studies. To this end, [28] applied this to the observed phase separation of 0.4 between the two peaks in the pulse profile of 1E 1841-045 within the energy range of 20-35 keV. We found that for $\gamma_e \sim 10$ that would result from strong cooling, this suggests that $\alpha \lesssim 20^\circ$, an estimate that is quite similar to the value of $\alpha \sim 15^\circ$ inferred in the analysis of [29]. This determination would change if toroidal components to the equatorial field (scattering locales that dominate the spectral signal) yield twist angles $\Delta\phi \sim 1$, i.e., significantly larger than those found at colatitudes $\theta > 60^\circ$ in MHD simulations of field untwisting [30].

In summary, the sample results presented here provide an idea of the constraints imposed upon our model, and a taste of the promise of the resonant Compton upscattering picture in explaining the phenomenon of the hard X-ray tails in magnetar quiescent emission. They also suggest the usefulness of the model in probing the magnetic angle α, thus aiding in reducing uncertainties in the determination of magnetar field strengths using spin-down information.

Acknowledgments
MGB acknowledges support by the NASA Astrophysics Theory (ATP) and *Fermi* Guest Investigator Programs through grants NNX13AQ82 and NNX13AP08G. ZW is supported by the South African National Research Foundation. PLG thanks the Michigan Space Grant Consortium, the National Science Foundation (grant AST-1009731), and NASA ATP through grant NNX13AO12G. AKH. also acknowledges support through the NASA ATP program.

References

[1] Kouveliotou C *et al* 1998 *Nature* **393** 235
[2] Duncan R C Thompson C 1992 *ApJ* **392** L9
[3] Thompson C and Duncan R C 1996 *ApJ* **473** 332
[4] Turolla R, Zane S and Watts A L 2015 *Reports on Progress in Physics* **78** 116901
[5] Kaspi V M and Beloborodov A M 2017 *Ann. Rev. Astron. Astrophys.* **55** 261
[6] Coti Zelati F, Rea N, Pons J, Campana S and Esposito P 2017, *Preprint* 1710.04671
[7] Hurley K *et al* 1999 *Nature* **397** 41
[8] Palmer D M *et al* 2005 *Nature* **434** 1107
[9] Kulkarni S R *et al* 2003 *ApJ* **585** 948
[10] Viganò D *et al* 2013 *MNRAS* **434** 123
[11] Kaspi V M *et al* 2003 *ApJ* **588** L93
[12] Lin L *et al* 2011 *ApJ* **740** L16
[13] Olausen S A and Kaspi V M 2014 *ApJS* **212** 6
[14] Kuiper L, Hermsen W and Mendeź M 2004 *ApJ* **613** 1173
[15] den Hartog P R *et al* 2008a *A&A* **489** 245
[16] Götz D *et al* 2006 *A&A* **449** L31
[17] Enoto T *et al* 2010 *ApJ* **722** L162
[18] Abdo A A *et al* 2010 *ApJ* **714** 927
[19] Li J, Torres D F, de Oña Wilhelmi E, Rea N and Martin J 2017 *ApJ* **835** 54
[20] Baring M G and Harding A K 2007 *Astr. Space Sci.* **308** 109
[21] Fernández R and Thompson C 2007 *ApJ* **660** 615
[22] Daugherty J K and Harding A K 1986 *ApJ* **309** 362
[23] Gonthier P L *et al* 2000 *ApJ* **540** 907
[24] Baring M G, Wadiasingh Z and Gonthier P L 2011 *ApJ* **733** 61
[25] Ho C and Epstein R I 1989 *ApJ* **343** 227
[26] Beloborodov A M 2013 *ApJ* **762** 13
[27] Gonthier P L *et al* 2014 *Phys. Rev.* D **90** 043014
[28] Wadiasingh Z, Baring M G, Gonthier P L and Harding A K 2017 *ApJ* submitted
[29] An H *et al* 2015 *ApJ* **807** 93
[30] Chen A Y and Beloborodov A M 2017 *ApJ* **844** 133